Electronic Supplementary Material (ESI) for ChemComm.

Tuning the chaotropic effect as an assembly motif through one-electron transfer in rhenium cluster

Anton A. Ivanov,[a,b,c] Clément Falaise,[a] David Landy,[d] Mohamed Haouas,*[a] Yuri V. Mironov,[b,e]
Michael A. Shestopalov [b,c,e] and Emmanuel Cadot*[a]

---

[a] *Institut Lavoisier de Versailles, CNRS, UVSQ, Université Paris-Saclay, Versailles, France.*
[b] *Nikolaev Institute of Inorganic Chemistry SB RAS, Novosibirsk, 630090, Russia.*
[c] *The Federal Research Center of Fundamental and Translational Medicine, Novosibirsk, 630117 Russia.*
[d] *Unité de Chimie Environnementale et Interactions sur le Vivant (UCEIV, EA 4492), ULCO, Dunkerque, France.*
[e] *Novosibirsk State University, Novosibirsk, 630090, Russia.*

Table of Content

1- Experimental Details

Synthesis: The compounds described herein, $K_4[\{\mathbf{Re_6red}@2\gamma\text{-CD}\}\cdot\gamma\text{-CD}]\cdot40H_2O$, $K_3[\{\mathbf{Re_6ox}@2\gamma\text{-CD}\}\cdot\gamma\text{-CD}]\cdot33H_2O$, and $K_6[\{\mathbf{Re_6ox}@2\gamma\text{-CD}\}\cdot\mathbf{Re_6ox}]\cdot23H_2O$, were synthesized from aqueous mixtures of gamma-cyclodextrin (TCI, 99%) and $K_4[Re_6Se_8(CN)_6]$. The starting chemical reactants were commercially available and were used without any further purification except $K_4[Re_6Se_8(CN)_6]$ which was synthesized as described in literature.[1] The synthesis of $K_4[\{\mathbf{Re_6red}@2\gamma\text{-CD}\}\cdot\gamma\text{-CD}]\cdot40H_2O$ has been already reported.[2]

$K_3[\{Re_6Se_8\}(CN)_6]\cdot EtOH$ noted $K_3\mathbf{Re_6ox}$: 10 ml of a Br_2 solution in acetonitrile (~ 0.2 M) was added to the powder $K_4[\{Re_6Se_8\}(CN)_6]$ (0.3 g, 0.145 mmol) and reaction mixture was stirred for 30 minutes. The dark green powder was separated from the solution on a porous filter and washed several times with acetonitrile. Then, the resulting complex was dissolved in 50 ml of ethanol, filtered and evaporated to dryness on a rotary evaporator. Yield: 0.286 g (95 %). EDS shows Re : Se : K ratio = 6 : 7.9 : 3.1. TGA revealed a weight loss of about 2.2% from 40 to 100 °C (the calculated weight loss of 1 EtOH is 2.2%).

$K_3\{[\{Re_6Se_8\}(CN)_6]\subset(\gamma\text{-CD})_2\}\cdot(\gamma\text{-CD})\cdot33H_2O$ noted **1**: Complex was obtained by two ways: 1) $K_3[\{Re_6Se_8\}(CN)_6]\cdot EtOH$ (0.202 g, 0.097 mmol) and γ-CD (0.407 g, 0.289 mmol) were dissolved in 5 mL of water. Final solution was allowed to slowly evaporate which gave green crystals of $K_3\{[\{Re_6Se_8\}(CN)_6]\subset(\gamma\text{-CD})_2\}\cdot(\gamma\text{-CD})\cdot33H_2O$; 2) $K_4[\{Re_6Se_8\}(CN)_6]$ (0.2 g, 0,097 mmol) and γ-CD (0.407 g, 0.289 mmol) were dissolved in 5 mL of water. Then, few drops of KBr/Br_2 solution in water (~ 0.2 M) were added to reaction mixture resulting in dark green solution Final solution was allowed to slowly evaporate which gave green crystals of $K_3\{[\{Re_6Se_8\}(CN)_6]\subset(\gamma\text{-CD})_2\}\cdot(\gamma\text{-CD})\cdot33H_2O$. Yield 0.51 g (81 %) based on cluster complex. Anal. Calcd for $C_{150}H_{306}K_3N_6O_{153}Re_6Se_8$: C, 27.62; H, 4.73; N, 1.29. Found: C, 27.5; H, 4.5; N, 1.3. EDS shows Re : Se : K ratio = 6 : 8.1 : 3.0. TGA revealed a weight loss of about 9.0% from 50 to 160 °C (the calculated weight loss of 33 H_2O is 9.1%).

$K_3\{[\{Re_6Se_8\}(CN)_6]\subset(\gamma\text{-CD})_2\}\cdot K_3[\{Re_6Se_8\}(CN)_6]\cdot23H_2O$ noted **2**: Complex was obtained by two ways: 1) $K_3[\{Re_6Se_8\}(CN)_6]\cdot EtOH$ (0.202 g, 0.097 mmol) and γ-CD (0.136 g, 0,097 mmol) were dissolved in 5 mL of water. Final solution was allowed to slowly evaporate which gave green crystals of $K_3\{[\{Re_6Se_8\}(CN)_6]\subset(\gamma\text{-CD})_2\}\cdot K_3[\{Re_6Se_8\}(CN)_6]\cdot23H_2O$; 2) $K_4[\{Re_6Se_8\}(CN)_6]$ (0.2 g, 0,097 mmol) and γ-CD (0.136 g, 0,097 mmol) were dissolved in 5 mL of water. Then, few drops of KBr/Br_2 solution in water (~ 0.2 M) were added to reaction mixture resulting in dark green solution Final solution was allowed to slowly evaporate which gave green crystals of $K_3\{[\{Re_6Se_8\}(CN)_6]\subset(\gamma\text{-CD})_2\}\cdot K_3[\{Re_6Se_8\}(CN)_6]\cdot23H_2O$. Yield 0.25 g (73 %) based on cluster complex. Anal. Calcd for $C_{108}H_{206}K_6N_{12}O_{103}Re_{12}Se_{16}$: C, 18.32; H, 2.93; N, 2.38. Found: C, 18.5; H, 3.0; N, 2.4. EDS shows Re : Se : K ratio = 6 : 8.1 : 3.0. TGA revealed a weight loss of about 6.0% from 50 to 160 °C (the calculated weight loss of 23 H_2O is 5.9%).

Single Crystal X-ray Diffraction: Crystals of compounds **1** and **2** were selected under polarizing optical microscope and glued in paratone oil to prevent any loss of crystallization water. X-ray intensity data were collected at low temperature (T = 200(2) K) on a Bruker D8 VENTURE diffractometer equipped with a PHOTON 100 CMOS bidimensional detector using a high brilliance IµS microfocus X-ray Mo K_α monochromatized radiation (λ = 0.71073 Å). Data reduction was accomplished using SAINT V7.53a. The substantial redundancy in data allowed a semi-empirical absorption correction (SADABS V2.10) to be applied, on the basis of multiple measurements of equivalent reflections. Using Olex2,[3] the structure was solved with the ShelXT[4] structure solution program using Intrinsic Phasing and refined with the ShelXL[5] refinement package using Least Squares minimization. The remaining non-hydrogen atoms were located from Fourier differences and were refined with anisotropic thermal parameters. Positions of the hydrogen atoms belonging to the cyclodextrins were calculated. Crystallographic data for single-crystal X-ray diffraction studies are summarized in Table S1. CIF files can be obtained free of charge from the Cambridge Crystallographic Data Centre via https://www.ccdc.cam.ac.uk. Deposit number: 1937126 for **1**, and 1937127 for **2**.

*Comments about the refinement of **1**:* The crystal structures reveal the presence of large voids which contain water molecules (H_2O) and potassium cations disordered. Thereby the contribution of solvent-electron density was removed using the SQUEEZE routine in PLATON, producing a set of solvent-free diffraction intensities.

*Comments about the refinement of **2**:* The crystal structures reveal the presence of large voids which contain water molecules (H_2O) and counter cations disordered. Only few of them can be located using crystallographic data. Thereby the contribution of solvent-electron density was removed using the SQUEEZE routine in PLATON, producing a set of solvent-free diffraction intensities. Using the option “Calc Solv” implemented in Platon (calculation done considering the host-guest complexes), we determined about 45% of the unit cell volume is accessible for water molecules. The crystal structure refinement of ***2-I*** reveals that one free oxidized cluster is disordered on two positions (50%/50%) and the cluster involved in host-guest inclusion complex is also disordered on two positions (82.5%/17.5%).

NMR studies. All NMR spectra were measured in D_2O at 27 °C. ^1H NMR spectra were recorded on a 400.13 MHz spectrometer (Bruker, Germany) at a field strength of 9.40 T. Chemical shifts were referenced to TMS. The transverse and longitudinal relaxation times, T_2 and T_1, of CD protons in the studied solutions were measured using the classical Carr-Purcell-Meiboom-Gill (CPMG) and inversion recovery pulse sequences. The inversion-recovery method using 180°-τ-90° pulse sequence was performed to determine T_1. T_2 was measured with CPMG sequence employing a 90°-180° pulses train. The 90° pulse was 8.5 μs in length. One scan was acquired for each measurement. For each experiment, 12 data points were collected for fitting. The repetition delay was chosen to be at least five times T_1. The dead time was 75 μs.

Electrochemistry. Cyclic voltammetric (CV) experiments were carried out with a Methrom Autolab PGSTAT230 driven by a computer using NOVA software. Measurements were performed at room temperature in a conventional single compartment cell. A glassy carbon (GC) electrode with a diameter of 3 mm was used as the working electrode. The auxiliary electrode was a Pt plate placed within a fritted-glass isolation chamber and potentials are quoted against a saturated calomel electrode (SCE). The solutions were deaerated thoroughly for at least 10 minutes with pure argon.

Energy-Dispersive X-ray Spectroscopy. EDS measurements were performed using a SEM-FEG (Scanning Electron Microscope enhanced by a Field Emission Gun) equipment (JSM 7001-F, Jeol). The measurements were acquired with a SDD XMax 50 mm^2 detector and the Aztec (Oxford) system working at 15 kV and 10 mm distance. The quantification is realized with the standard library provided by the constructor using Lα lines.

2- Single-Crystal X-Ray Diffraction

2.1- Crystallographic Parameters

Table S1: Selected crystallographic parameters of the single-crystal X-ray diffraction structural analysis

Compound	**1**	**2**
Empirical formula	$C_{150}H_{156}N_6O_{144}Re_6Se_8$	$C_{111}H_{109}K_{2.5}N_{15}O_{80}Re_{15}Se_{20}$
Formula weight	6127.68	7403.08
Temperature/K	200(2)	200(2))
Crystal system	tetragonal	orthorhombic
Space group	*I*422	$P2_12_12$
***a, b, c* /Å**	23.8167(14) 23.8167(14) 57.132(4)	35.247(4) 35.747(4) 17.7344(17)
***α, β, γ* /°**	90 90 90	90 90 90
Volume/Å^3	32408(4)	22345(4)
Z	4	4
ρ_{calc}g/cm^3	1.256	2.201
μ/mm^{-1}	3.211	11.467
F(000)	11952.0	13490.0
Crystal size/mm^3	0.2 × 0.17 × 0.17	0.12 × 0.11 × 0.04
Radiation	MoKα (λ = 0.71073)	MoKα (λ = 0.71073)
2Θ range for data collection/°	4.278 to 50.256	1.622 to 52.856
Index ranges	$-28 \leq h \leq 28$ $-28 \leq k \leq 28$ $-68 \leq l \leq 68$	$-44 \leq h \leq 44$ $-44 \leq k \leq 44$ $-22 \leq l \leq 22$
Reflections collected	282624	512434
Independent reflections	14443 R_{int} = 0.0800 R_{sigma} = 0.0314	45816 R_{int} = 0.1199 R_{sigma} = 0.0741
Data/restraints/parameters	14443/18/759	45816/0/ 891
Goodness-of-fit on F^2	1.085	1.034
Final R indexes [I>=2σ (I)]	R_1 = 0.0497, wR_2 = 0.1498	R_1 = 0.0819, wR_2 = 0.1885
Final R indexes [all data]	R_1 = 0.0676, wR_2 = 0.1657	R_1 = 0.1377, wR_2 = 0.2308
Largest diff. peak/hole / e Å^{-3}	1.86/-1.58	4.64/-5.08

2.2- Structural Description of Supramolecular Hybrid Compounds

Compound **1.** Structural analysis of $K_3[\{Re_6Se_8(CN)_6@(\gamma{-}CD)_2\}\cdot\gamma{-}CD]\cdot 33H_2O$ revealed to be isostructural to the reduced form based compound, $K_4\{[Re_6Se_8(CN)_6]@(\gamma\text{-}CD)_2\}\cdot(\gamma\text{-}CD)\cdot 40H_2O$ (K_4[{**Re_6red**@2γ-CD}·γ-CD]) which has been described in reference 2. Briefly, the cyanide rhenium cluster complex closely embedded within a cavity defined by two γ-CDs facing their secondary faces. Within this host-guest complex, the distances between the cyclodextrins are in the range of 2.8-3.1 Å (O···O). Packaging occurs due to the interaction of two inclusion compounds through the primary faces of the cyclodextrins along the [001] direction, forming a tubular structure (Fig. 36C). Also, the structures additionally contain a free CD (per inclusion complex), which closes on both sides the primary faces of the tubular structure (Figure S1a a). The crystal structure arrangement reveals the formation of large voids between the tubular fragments (Fig S1a b and c). The water molecules and disordered potassium cations are distributed within these large voids which represent almost 45% of the unit cell volume.

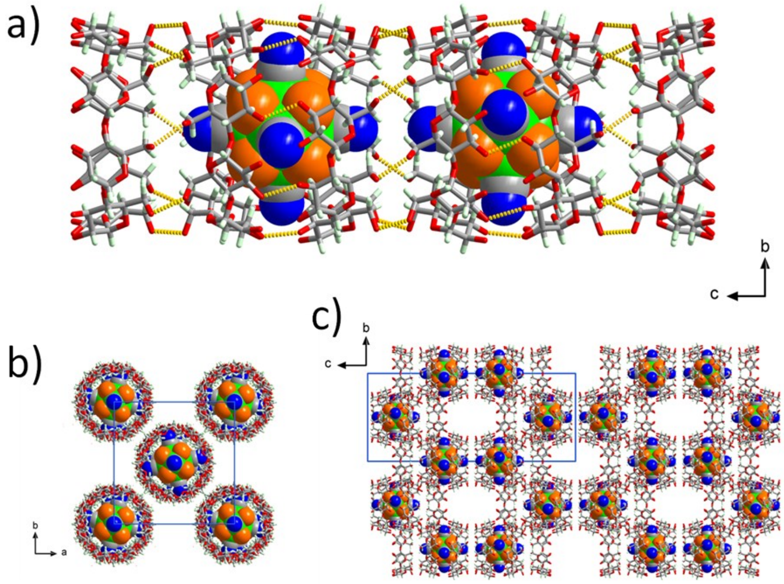

Figure S1a: a) Mixed representations of solid state structure of the compound **1** highlighting the close packing of clusters and CDs within a bamboo like arrangement. Hydrogen bonds between the hydroxyls of CDs are shown in yellow dashed line. b) Illustration of the packing viewed in the *ab* plane showing the tubular arrangement along *c* axis. c) The lattice viewed in the *bc* plane showing the presence of voids between the tubular motif built from the assembly of two clusters and 6 CDs. Color code: green=rhenium, orange= Se, grey=carbon, blue=nitrogen, red=oxygen, white=hydrogen.

Compound **2.** The crystallographic structural of $K_6\{[Re_6Se_8(CN)_6]@(\gamma\text{-}CD)_2\}\cdot(Re_6Se_8(CN)_6)\cdot 23H_2O$ consists of co-crystallization of a supramolecular complex constituted of the octahedral cluster $[Re_6Se_8(CN)_6]^{3-}$ closely embedded into two γ-CDs facing their wider rim (secondary face) together with a free and $[Re_6Se_8(CN)_6]^{3-}$ cluster (Fig S1b, a). The disposition of the cluster with respect to the γ-CD in the sandwich complexes $\{[Re_6Se_8(CN)_6]@(\gamma\text{-}CD)_2\}^{3-}$ is the same to that observed with the reduced form $\{[Re_6Se_8(CN)_6]@(\gamma\text{-}CD)_2\}^{4-}$ in compound **1**. The atomic distances in the reduced and oxidized forms are comparable (see Table S2). In the crystal packing, supramolecular adducts $\{[Re_6Se_8(CN)_6]@(\gamma\text{-}CD)_2\}^{3-}$ is decorated by eight free oxidized clusters, forming a pseudo-cube around the inclusion complex. In such arrangement the shortest distance between two adjacent neighboring clusters is about 7 Å. The packing of the inclusion complexes is quite intricate (Fig S1b, b). The inclusion complexes are stacked together in a zigzag fashion forming parallel corrugated chains of the adducts. At last, free uncomplexed clusters $\{Re_6Se_8(CN)_6\}^{3-}$ and potassium cations are positioned around the sandwich adducts filling the voids between these chains.

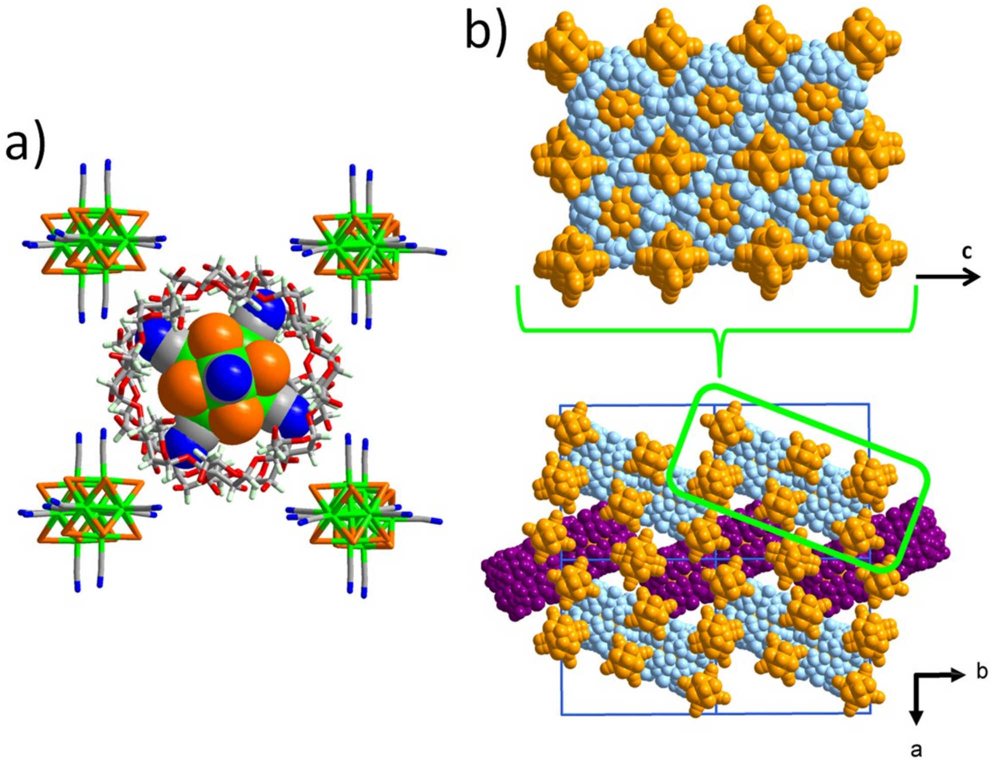

Figure S1b: Mixed representations of solid state structure of the compound **2** highlighting the arrangement of the inclusion complexes and free Re$_6$ clusters. a) Each inclusion complex is decorated by eight free clusters forming a pseudo cube .b) Illustration of the packing viewed in the *ab* plane.

Table S2: Bond distances of the encapsulated clusters [Re$_6$Se$_8$(CN)$_6$]$^{3/4-}$.

	Min/max, mean bond distances (Å)			
	2		**1**	[{[{Re$_6$**red**@2γ-CD}·γ-CD]
	Free cluster {Re$_6$**ox**}$^{3-}$	{Re$_6$**ox**@2γ-CD}$^{3-}$	{Re$_6$**ox**@2γ-CD}$^{3-}$	{ Re$_6$**red**@2γ-CD}$^{4-}$
Re-Re	2.5787 /2.66817 (2.6292)	2.5787 / 2.6817 (2.6292)	2.6222 / 2.6277 (2.6267)	2.6330 / 2.6351 (2.6341)
Re-Se	2.4771/ 2.58007 (2.5293)	2.4648 / 2.5744 (2.5253)	2.5107 / 2.5235 (2.5217)	2.5284 / 2.5343 (2.5308)
Re-C	2.0389 / 2.1349 (2.0999)	2.0181 / 2.1147 (2.1011)	2.0333 / 2.0826 (2.0193)	2.0285 / 2.1074 (2.0787)
C-N	1.1144 / 1.1802 (1.1393)	1.0700 / 1.2726 (1.1595)	1.1443 / 1.1821 (1.1645)	1.1375 / 1.2409 (1.1774)

3- NMR Relaxation Measurements

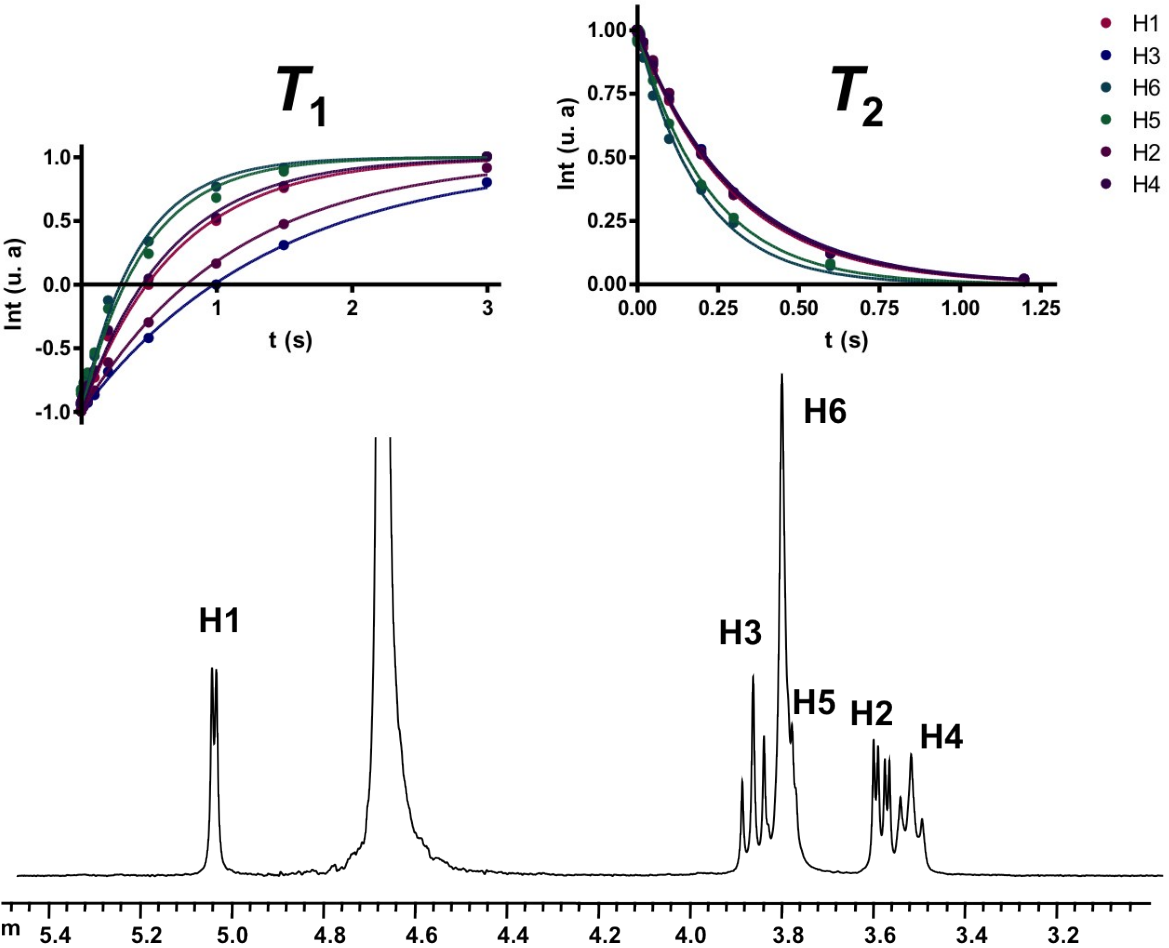

Figure S2: T_1 and T_2 relaxation time measurements of γ-CD protons in a 2 mM aqueous solution of γ-CD.

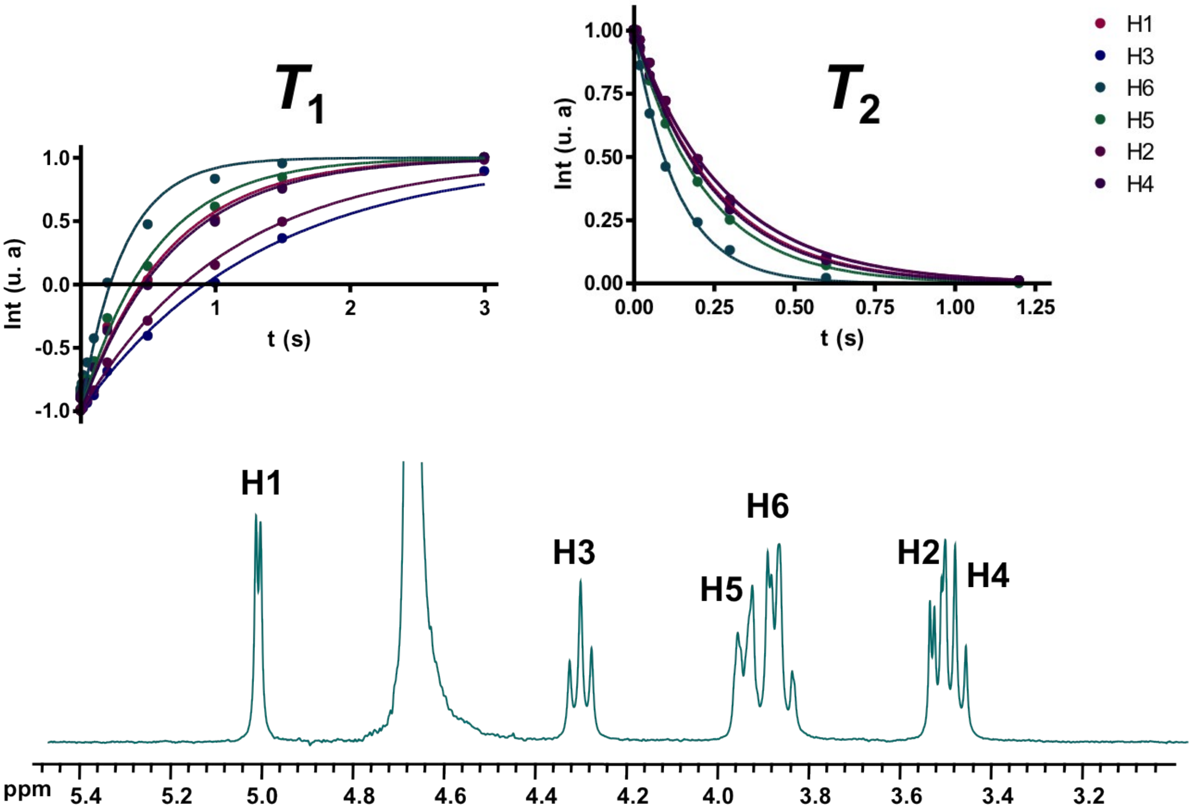

Figure S3: T_1 and T_2 relaxation time measurements of γ-CD protons in a 1 mM aqueous solution of [{**Re$_6$red**@2γ-CD}·γ-CD].

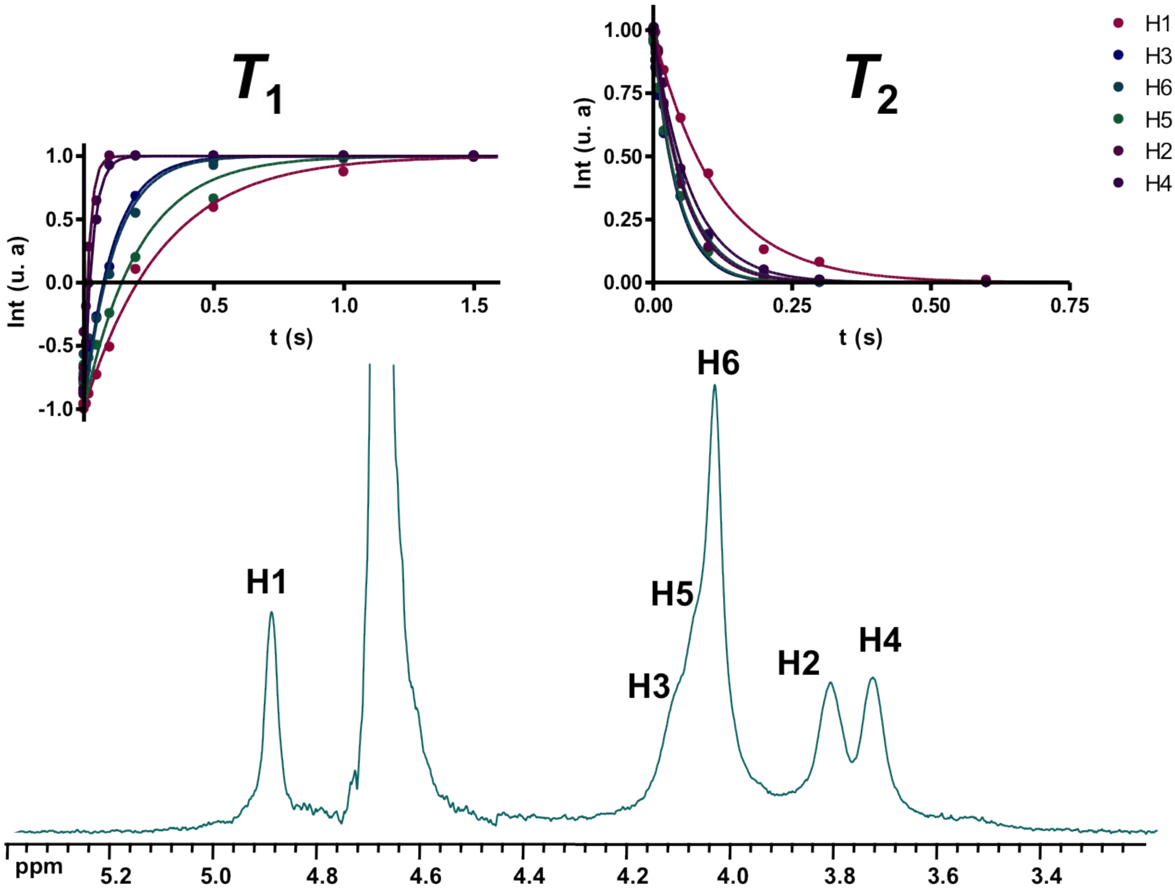

Figure S4: T_1 and T_2 relaxation time measurements of γ-CD protons in a 1 mM aqueous solution of [{**Re_6ox**@2γ-CD}·**Re_6ox**].

4- Isothermal Titration Calorimetry

Formation constants and inclusion enthalpies were simultaneously determined for the γ-CD/$K_3[Re_6Se_8(CN)_6]$ system by the use of an isothermal calorimeter (ITC_{200}, MicroCal Inc., USA), at three temperatures (283, 291 and 298 K), by means of classical titration experiments. Degassed water solutions were used in both cell (V_0 = 202.8 µL, filled with a 0.25mM $K_3[Re_6Se_8(CN)_6]$ solution) and syringe (40 µL, filled with a 5mM γ-CD solution). After addition of an initial aliquot of 1 µL, 20 aliquots of 1 µL of the syringe solution were delivered over 2 s for each injection. The time interval between two consecutive injections was 100 s, which proved to be sufficient for a systematic and complete return to baseline. The agitation speed was set to 750 rpm. The resulting heat flow was recorded as a function of time.

The heat of dilution of each partner was eliminated from each titration by subtracting the raw signal obtained for the corresponding blank titrations (i.e. only one partner in cell or syringe, the other compartment being filled with water). The peak area following each addition was obtained by integration of the resulting signal and was expressed as the heat effect per injection. Data corresponding to each first 1 µL injection were discarded from the fitting process. Binding constants and inclusion enthalpies were determined by nonlinear regression analysis of the binding isotherms, using a dedicated homemade program[6] (Excel spreadsheet).

Briefly, considering host and guest concentrations in syringe and in cell (before and after each injection), concentrations of each inclusion compound may be calculated by solving the binding polynomial corresponding to a mixture of 1:1 and 2:1 complexes**.** These concentrations may then be used to calculate the variation, in the cell, of the number of moles, Δn_i, of any CD_m-Cluster complex, for each injection, according to equation (1) :

$$\Delta n_i = \left[[CD_m\text{ - Cluster}]_i^{CELL} * V_o - [CD_m\text{ - Cluster}]_{i-1}^{CELL} * (V_o - v_i) + \frac{[CD_m\text{ - Cluster}]_i^{CELL} * v_i - [CD_m\text{ - Cluster}]_{i-1}^{CELL} * v_i}{2} \right] \qquad (1)$$

With v_i being the injected volume of the ith injection.

Finally, the heat consecutive to each injection may be calculated by means of relation (2) :

$$Q_i = \Delta n_i^{CD_1\text{ - Cluster}} * \Delta H^{CD_1\text{ - Cluster}} + \Delta n_i^{CD_2\text{ - Cluster}} * \left(\Delta H^{CD_1\text{ - Cluster}} + \Delta H^{CD_2\text{ - Cluster}}\right) \qquad (2)$$

It has to be stressed that $\Delta H^{CD_2\text{ - Cluster}}$ correspond to the formation of the 2:1 complex starting from the 1:1 complex (and not from the free species).

The fitting between experimental and theoretical heats was realized by means of Newton-Raphson algorithm, which minimizes the residual sum of squared deviations between experimental and theoretical data, by varying the thermodynamic parameters. In order to ensure that data treatment is not over-parameterized, a global analysis of the 3 titrations (283, 291 and 298 K) was realized. The least square fitting was simultaneously applied to all isotherms with one set of thermodynamic parameters (i.e. with a unique formation constant K, inclusion enthalpy $\Delta_r H$ and heat capacity variation $\Delta_r Cp$), by means of van't Hoff law. T_0 being an arbitrary reference temperature, $\Delta G(T)$, $\Delta_r H(T)$, $\Delta_r S(T)$ and $\Delta_r C_p$ are linked by equations (3) to (5) :

$$K(T) = K(T_0) * e^{\left\{\frac{\Delta_r H(T_0)}{R}\left(\frac{1}{T_0} - \frac{1}{T}\right) + \frac{\Delta_r C_p}{R}\left(\ln\left(\frac{T}{T_0}\right) + \frac{T_0}{T} - 1\right)\right\}} \qquad (3)$$

$$\Delta_r H(T) = \Delta_r H(T_0) + \Delta_r C_p * (T - T_0) \qquad (4)$$

$$\Delta_r G(T) = \Delta_r H(T) - T * \Delta_r S(T) \qquad (5)$$

Finally, uncertainties on each thermodynamic parameter were determined by a priori variance–covariance matrix[1]. Calculations of accuracy have been undertaken on real isotherms after global analysis. Table S3 summarizes the overall results of the three experiments (Figure S5).

Table S3: Formation constant, enthalpy, entropy and free energy of inclusion, for the 1:1 and 2:1 complexes formed between γ-CD and $K_3[Re_6Se_8(CN)_6]$, obtained from ITC data, at 283, 291 and 298 K. Uncertainty rounded to the superior unit.

	T (K)	K (10^3 M^{-1})	$\Delta_r H^*$ (KJ.mol^{-1})	TΔ_r S* (KJ.mol^{-1})	Δ_r G* (KJ.mol^{-1})
1:1	283	643.8 ± 65.5	-50.2 ± 0.2	-18.7 ± 0.5	-31.5 ± 0.2
1:1	291	360.3 ± 36.6	-49.2 ± 0.2	-18.2 ± 0.5	-31.0 ± 0.2
1:1	298	224.5 ± 22.8	-48.2 ± 0.2	-17.7 ± 0.5	-30.5 ± 0.3
2:1	283	3.2 ± 0.7	-17.1 ± 1.6	1.9 ± 2.1	-19.0 ± 0.5
2:1	291	2.6 ± 0.6	-19.1 ± 0.7	-0.1 ± 1.2	-19.0 ± 0.5
2:1	298	2.1 ± 0.5	-20.9 ± 0.8	-1.9 ± 1.4	-19.0 ± 0.5

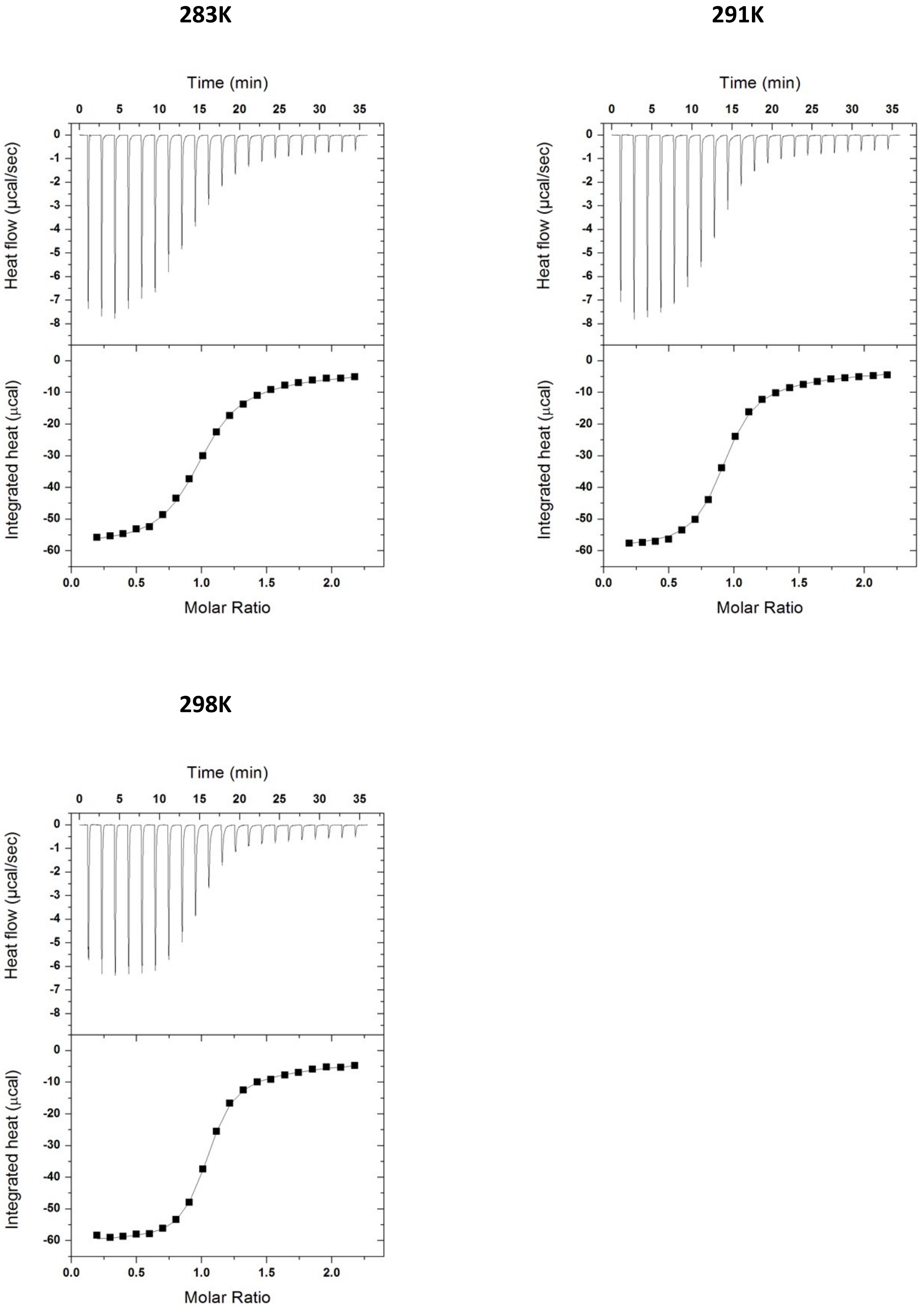

Figure S5: ITC thermograms (upper part) and isotherms (lower part) for the system γ-CD/$K_3[Re_6Se_8(CN)_6]$. Dots and lines correspond to experimental and theoretical heats, respectively.

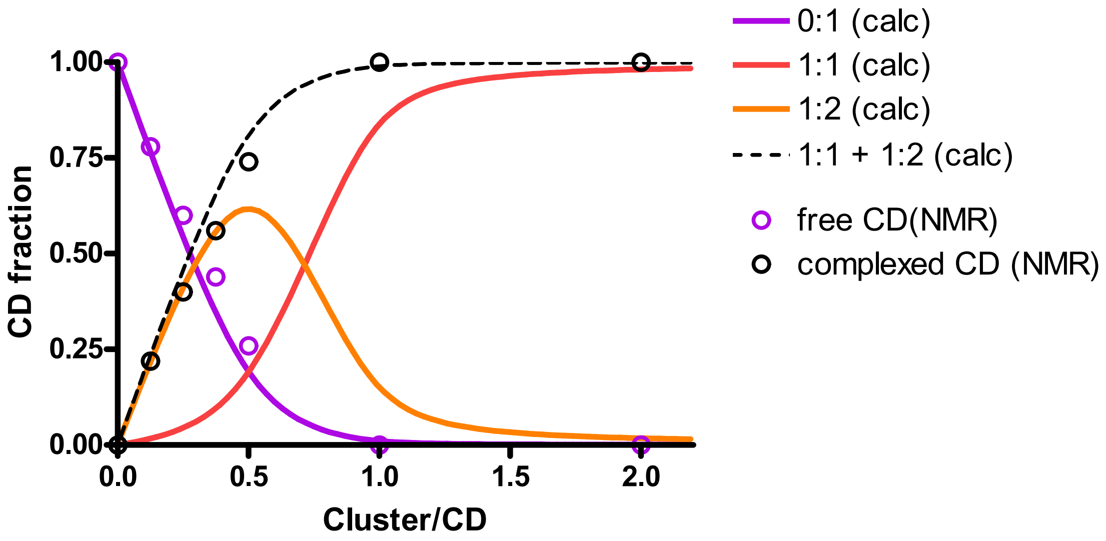

Figure S6: CD based species distribution as a function of cluster/CD molar ratio for the system γ-CD/$K_3[Re_6Se_8(CN)_6]$ at fixed [CD] = 4 mM. Dots and lines correspond to NMR (integration of H1 signals) and calculation from ITC data, respectively.

5- Electrochemistry

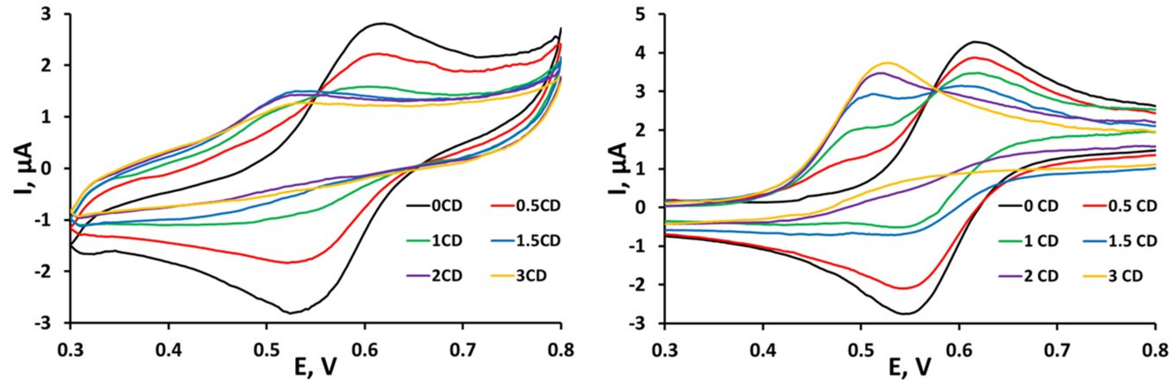

Figure S7: Cyclic voltammetry of the {Re$_6$**ox**}$^{3-}$ (left) and {Re$_6$**red**}$^{4-}$ (right) anions (0.5 mM, 25 mM $HClO_4$ aqueous solution, glassy carbon working electrode, scan rate 50 mV/s) in absence and presence of various amounts of γ-CD up to 3 equivalents

References:

1 N. G. Naumov, A. V. Virovets, N. V. Podberezskaya and V. E. Fedorov, *J. Struct. Chem.*, 1997, **38**, 857–862.

2 A. A. Ivanov, C. Falaise, P. A. Abramov, M. A. Shestopalov, K. Kirakci, K. Lang, M. A. Moussawi, M. N. Sokolov, N. G. Naumov, S. Floquet, D. Landy, M. Haouas, K. A. Brylev, Y. V. Mironov, Y. Molard, S. Cordier and E. Cadot, *Chem.-Eur. J.*, 2018, **24**, 13467–13478.

3 O. V. Dolomanov, L. J. Bourhis, R. J. Gildea, J. a. K. Howard and H. Puschmann, *J. Appl. Crystallogr.*, 2009, **42**, 339–341.

4 G. M. Sheldrick, *Acta Crystallogr. Sect. Found. Adv.*, 2015, **71**, 3–8.

5 G. M. Sheldrick, *Acta Crystallogr. Sect. C Struct. Chem.*, 2015, **71**, 3–8.

6 E. Bertaut and D. Landy, *Beilstein J. Org. Chem.,* 2014, **10**, 2630-2641.